An AI-Based Modelling of a Sorption Enhanced Chemical-Looping Methane Reforming Unit

Salehi, Reza
Department of Civil, Chemical, Environmental and Materials Engineering, University of Bologna, Bologna, ITALY

Rahimzadeh, Hassan
Department of Biosystems Engineering, Isfahan University of Technology, Isfahan, I.R. IRAN

Heidarian, Pouria
Energy Department, Politecnico di Milano, Milan, ITALY

Salimi, Farhad*+
Department of Chemical Engineering, Kermanshah Branch, Islamic Azad University, Kermanshah, I.R. IRAN

ABSTRACT: *Hydrogen as a green fuel has attracted enormous attention recently. Although hydrogen combustion produces no harmful by-products, hydrogen production can be almost disastrous. Hydrogen production mainly originates from fossil fuels, and more than 80% of hydrogen production is produced using fossil fuel reformation with CO_2 formation as a by-product. Light hydrocarbon gases, predominantly methane, are extensively used for hydrogen production. While methane reforming is an economical and efficient process, decarburization of flue gas can be a challenge. Processes involving chemical looping can be used to mitigate these challenges, and they are favorable for simultaneous CO_2 capture during hydrogen generation. Intelligent models can help have accurate monitoring of such plants. The aim of this paper is to provide an Artificial Intelligence (AI) based approach to model a Sorption-Enhanced Chemical-Looping Reforming (SECLR) unit. To this end first, a SECLR unit was simulated using ASPEN Plus version 11. Then the simulation results were validated by experimental data, and the SECLR unit went through 31000 different scenarios. The derived data from ASPEN Plus was modeled and simulated with machine learning methods to estimate the CH_4 conversion, H_2 Purity, and CO_2 removal in the SECLR process. Artificial neural networks, ensemble learning, and support vector machine methods were developed to predict the CH_4 conversion, H_2 Purity, and CO_2 removal in a SECLR unit. All three models could provide satisfactory results for predicting CH_4 conversion, CO_2 removal, and H_2 Purity. According to statistical evaluations, Artificial Neural Network (ANN) outperformed Support Vector Machine (SVM) and ensemble learning in producing results with lower error values and higher accuracy with an average 5.23e-5 of error and R^2 of 0.9864.*

KEYWORDS: *Machine learning; Methane reforming; Artificial neural network; Chemical-looping reforming; Ensemble learning.*

**To whom correspondence should be addressed*
+ *E-mail: f.salimi@iauksh.ac.ir*
1021-9986/2023/7/2079-2089 11/$/6.01

INTRODUCTION

Various hydrocarbons can be exploited to produce hydrogen via reforming reactions. Hydrogen can be an essential component for various applications [1], for instance, as a feed in the production of many chemicals such as ammonia and fertilizers, as well as in the refining industry. Hydrogen is also regarded as the fuel of the future[2]. The only product of hydrogen combustion is water. Therefore, the problems with fossil fuel inflammation, such as greenhouse gases and pollutants emissions, can be assuaged drastically. Hydrogen is mainly produced via methane steam reforming reaction. However, hydrocarbon reforming units can also be CO_2-producing spots [3, 4]. Globally increasing of energy demand led to a rise in energy consumption by gas and oil companies. Thus, this increased demand leads to more emission of CO_2 [5]. Iran contains significant sections of oil and gas industries which rank Iran as the 7th country with the most pollutants in industry[6]. An environment-friendly approach to producing hydrogen is the synchronous production of hydrogen alongside a CO_2 capture unit. Processes containing chemical looping such as Chemical-Looping Reforming (CLR), Sorption-Enhanced (SE) reforming, and a hybrid method of these two methods (SECLR) can provide such an approach [7-11]. The principle of chemical-looping is based on methane oxidation via cyclic reduction and oxidation of a solid oxygen carrier. The separation of products from nitrogen can be costly; therefore, in this method, the products are not mixed with the nitrogen in the air [10]. Chemical-looping process also includes other cyclic reactions between solids and gases. One such cycle is the calcium looping, in which calcium oxide (CaO) as an oxygen carrier is calcinated and carbonated with CO2. This hybrid process facilitates the production of hydrogen alongside a CO_2 capture unit without needing further separation after the accomplishment of the reactions [12]. Precise assessment is an irresolvable segment of a hydrogen production plant. Machine learning methods have been proven to be efficacious in evaluating the performance of SECLR units [13]. *Norouzi et al* [14-27] studied CO_2 capture in a variety of industrial cases. They reported the energetic analysis of a SMR reactor along with CO_2 turbine, heavy oil thermal conversion using formic acid followed by a CO_2 capture process, and simulation of methane gas production process from animal waste in a reactor. *Shalaby et al.* [28] proposed a machine learning approach for optimizing and modeling CO_2 post-combustion units. They developed machine learning models to predict outputs of a post-combustion unit and developed a fine tree, Matern Gaussian Process Regression (GPR), rational quadratic GPR, and squared exponential GPR models and compared the results of these methods with a feed-forward ANN model. Also, they used Genetic Algorithms (GA) and Sequential Quadratic Programming (SQP) to optimize operating parameters *Bai et al.* [29] developed a machine learning model for post-combustion CO_2 capture with the bootstrap aggregated Extreme Learning Machine (ELM) to predict CO_2 capture rate and CO_2 capture level. *Valera et al.* [30] developed an ANN for the estimation of the volumetric mass transfer coefficient of a spray tower. In their simulation, the gas flow rate was variable, and the other conditions were constant. They employed many different training algorithms and transfer functions and claimed that ANN could be used efficiently to predict essential variables. *Li et al.* [13] developed an ANN to assess the performance of a post-combustion CO_2 capture unit. They developed their model under steady and unsteady states. ANN was employed to predict CO_2 capture rate and CO_2 capture level in their work. To our knowledge and reviewing literature enlightened that an AI-based study of SECLR unit has not been accomplished yet. In this work, the SECLR unit was simulated via ASPEN Plus version 11 and then validated by experimental data reported by *Ryden et al*. [31]. Afterward, the validated model has undergone 31000 different scenarios. Then, using the obtained data of various scenarios, data-based models, namely ANN, SVM, and ensemble learning, were developed to predict CH_4 conversion, H_2 Purity, and CO_2 removal of a SECLR unit. MATLAB® software (version 2014b) was employed to develop these intelligent models. Finally, the performance of the proposed machine learning methods was reported and compared. Scheme 1 indicates the Overall flowchart of the simulation, validation, and developing AI methods.

Methodologies

ASPEN Plus

Simulation of a SECLR unit was accomplished *via* ASPEN Plus version 11. Fig. 1 shows a schematic of the process flowsheet in Aspen Plus software.

To develop the model following assumptions were assumed:

Table1: Blocks of Aspen Plus flowsheet

Blocks name in Aspen Flowsheet	Apparatus
HX1	Counter-current shell & tube heat exchanger
HX2	Counter-current shell & tube heat exchanger
HX3	Counter-current shell & tube heat exchanger
FUEL-REA	Rgibbs reactor
CAL-REA	Rgibbs reactor
AIR-REA	Rgibbs reactor
CYCLON1	Gas-solid cyclone separator
CYCLON2	Gas-solid cyclone separator
CYCLON3	Gas-solid cyclone separator

- The process is steady-state.
- Thermodynamic equilibrium is reached in all of the reactors, FUEL-REA (Fuel reactor), CAL-REA (Calcination reactor), and AIR-REA (Air reactor).
- The separation between solids and gas in all of the cyclones (CYCLON1, CYCLON2, and CYCLON3) is perfect.

Table 1 indicates the name and abbreviations for all of the blocks in the process flowsheet.

In this simulation, the reactant stream (CH_4 and H_2O), before entering the reforming reactor (FUEL-REA), is preheated isothermally through heat exchangers (HX1, HX2, and HX3). Although the desired product of methane steam reforming is hydrogen, other species in the reforming reactor output stream are CH_4, H_2O, CO, $CaCO_3$, and Ni. To separate the Ni and $CaCO_3$ from gas, the reforming reactor output stream (H_2+Solids) is carried to a cyclone (CYCLONE1). The stream of hydrogen (HTOH2) passes through a heat exchanger (HX1) where it cools and preheats the reactant stream. To calcine $CaCO_3$ into CaO and CO_2 stream (Ni+ $CaCO_3$) is carried to a calcination reactor (CALCINA). A cyclone (CYCLONE2) is used to separate CO_2 gas from the solids of the (CO_2+SOLI) stream. The separated CO_2 is passed through a heat exchanger (HX2) to further preheat the reactant stream. To form NiO as an oxygen carrier, the stream (NI +CAO) is carried to a reactor (AIR-REA) where the Ni reacts adiabatically with air. To separate N_2 from the solids stream (CaO+NiO) is fed to a cyclone (CYCLONE3). The solids are subsequently fed to the fuel reactor as stream NIO–CAO. The hot N_2 in stream N_2, is passed through a heat exchanger (HX3), exchanging heat with feed (REACTANT2). The feed stream is heated up to the reactor temperature and then is fed to the reactor (FUEL-REA). Reactions occur in the RGIBBS reactor, which is based on the minimization of Gibbs free energy. Total Gibbs energy of a reaction system is expressed as following [7]:

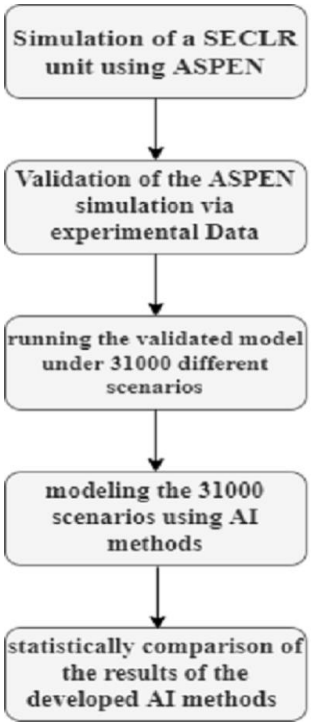

Schem.1: Overall flowchart of the simulation, validation, and developing AI methods

$$G_{total} = \sum_{i=1}^{N} n_i \mu_i \quad (1)$$

Where $\boldsymbol{\mu_i}$the chemical potential of chemical species and n indicates the number of moles of chemical.

$$\mu_i = \mu_i^0 + RT \ln \frac{y_i \varphi_i P}{P_0} = \mu_i^0 + RT \ln a_i \quad (2)$$

Where μ_i^0 is the pure ideal gas standard chemical potential. *yi* and $\varphi_i$are the vapor molar fraction and the fugacity coefficient of a species in a mixture, respectively. We consider *P* and P_0 as the overall and reference pressures in a given temperature, respectively. Substituting Eq. (2) in Eq. (1) gives:

$$G_{total} = \sum_{i=1}^{N} n_i \mu_i^{\,0} = \sum_{i=1}^{N} n_i RT \ln \alpha_i \quad (3)$$

Table 2: Validation of simulation results with Ryden et al. [31] results

Flow rate (mol/hr)	Simulation	Reference	Deviation (%)
Fuel Reactor product gas			
CH_4	0.02908	0.030	3.06
H_2O	1.265	1.328	4.74
H_2	2.87	2.811	2.098
CO_2	0.009378	0.011	14.7
CO	0.007020	0.008	12.25
H_2 Purity	98.44	98.7	0.26
CH_4 Conversion	97	97	0
Calciner product gas			
CO_2	0.95452	0.95	4.747

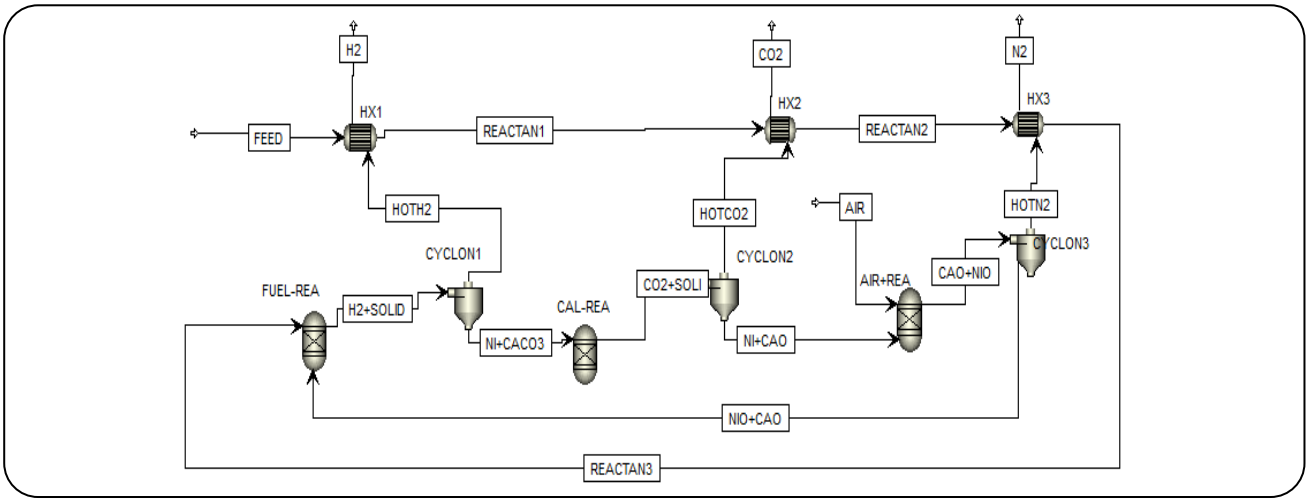

Fig. 1: schematic of process flowsheet in Aspen Plus

Where, α_i is the activity term. In order to minimize Gibbs free energy, one should find n_i values in Eq. (3) that minimizes the Gibbs free energy restricted to the following term:

$$\sum_{i=1}^{N} a_{ij} n_i = A_j \quad (4)$$

Where a_{ij} is the number of "j" species in a mole of "i" species, A_j is the total number of atoms of jth species in the reaction environment. Lagrange multiplier method can minimize the Gibbs free energy as following [9]:

$$\frac{\partial L}{\partial n_i} = \Delta G_{f,i}^{0} + RT \ln \alpha_i + \sum_{i=1}^{k} \lambda_i a_{ij} = 0 \quad (5)$$

Where, λ_i and L are the Lagrange multiplier and the Lagrange function, respectively. The result of the simulated model was validated with the experimental results. The operating conditions for the validation are as follows. The molar flow ratio of methane to steam is 1:2.2 mol and the temperature of the steam is 312℃ and the temperature of fuel rector is 580℃. The temperature and pressure of the calcination reactor are 880℃ and 1 bar, respectively. Table 2 shows validated results.

The average deviation of simulation results from reference results is 5.3 % which is negligible and shows that simulation has been accomplished appropriately.

In order to make a reliable dataset for machine learning methods, 31252 different scenarios have been executed on the simulated Aspen Plus model. Table 3 shows the operational parameters and their ranges.

The selected range for the operational parameters were chosen according to the literature. The operational parameters are Temperature [℃], pressure [bar], steam flowrate [kmol/h], methane flowrate [kmol/h], CaO flowrate[kmol/h], and NiO flowrate [kmol/h], and outputs are CH_4 conversion (%), H_2 Purity (%) and CO_2 removal (%). The model has been operated under different operational parameters, and these parameters have changed continuously to make different scenarios.

Table 3: Operational parameters and outputs range

Parameter	Type	Range	First point	Mid-point	End point
Temperature [℃]	Input	500-675	500	587.5	675
Pressure [bar]	Input	1-5	1	3	5
Steam flowrate [kmol/hr]	Input	0.0035-0.005	0.0035	0.00425	0.005
Methane flowrate [kmol/hr]	Input	0.001-0.0015	0.001	0.00125	0.0015
CaO flowrate [kmol/hr]	Input	0.001-0.0013	0.001	0.00115	0.0013
NiO flowrate [kmol/hr]	Input	0.001-0.0014	0.001	0.0012	0.0014
CO_2 removal (%)	output	0.7638- 0.9998	0.7638	0.8818	0.9998
H_2 Purity (%)	output	0.8402- 0.9991	0.8402	0.91965	0.9991
CH_4 Conversion (%)	output	0.6690-0.9993	0.6690	0.83415	0.9993

To determine the accuracy of developed ML methods to predict the CH_4 conversion, CO_2 Purity and H_2 purity of a SECLR unit statistical measures, namely coefficient of determination (R^2), Mean Squared Error (MSE), and Root Mean Squared Error (RMSE) were calculated as follows:

$$R^2=1-\frac{\sum_{i=1}^{n}[x_i^{pre}-x_i^{exp}]^2}{\sum_{i=1}^{n}[x_i^{pre}-x_i^{m}]^2} \quad , \quad x_m=\frac{\sum_{i=1}^{n}x_i^{exp}}{n} \tag{6}$$

$$MSE=\frac{1}{n}\sum_{i=1}^{n}[x_i^{exp}]^{pre^2} \tag{7}$$

$$\mathbf{R}MSE=\sqrt{\frac{1}{n}\sum_{i=1}^{n}[x_i^{exp}]^{pre^2}} \tag{8}$$

Where x_i^{exp}, x_i^{pre} are experimental and predicted values, respectively, and *n* indicates the number of data points.

Intelligent models

In this paper, three machine learning methods, namely ANN, Ensemble learning, and SVM, were employed to predict CH_4 conversion, H_2 Purity and CO_2 removal of a SECLR unit. 31252 different scenarios were considered as 31252 datapoints and were normalized between 0 and 1 before the implantation of the machine learning methods. Moreover, 70 % of the data points were selected randomly as a training set to build the intelligent models, and 30 % were selected as the test set to test the precision of the developed models.

Artificial neural network

Artificial neural networks imitated from the principles of biological neural network function establishes a regression amongst independent variables and dependent variables and extracts delicate information and complex knowledge from the representative data set. ANN structure consists of an input layer, one or more hidden layers, and one output layer [32]. Fig 2a depicts a schematic of an ANN. In the developed model, the Levenberg-Marquardt algorithm, an approximation of Newton's method, was used as the training algorithm. A hidden layer comprising 30 neurons was applied, and hyperbolic tangent sigmoid and linear function (purelin) was used as the transfer functions between the layers.

Support vector machine

A SVM is a supervised learning method famous for employing it in classification and regression issues. SVM creates a set of hyperplanes to classify and regress all inputs in a high-dimensional space. The closest patterns to the classification and regression margin are called support vectors. The objective of an SVM is to maximize the margin between the hyperplane and the support vectors. For nonlinear problems, SVM creates a set of patterns and a feature space in which the initial nonlinear boundaries are linearly separable by mapping the features' space. This mapping is done by a set of mathematical core functions called kernels. SVM algorithm is also utilized for multivariate regression problems. As for classification, when the SVM is applied for regression, the algorithm contains the main features that characterize the maximum margin algorithm[33]. For the regression, the SVM looks for a feasible solution by individualizing the hyperplane that maximizes the margin. However, since the final predicted value is an actual number, the tolerance of the error is more flexible. The SVM can be performed linear or nonlinearly, depending on the applied kernel function.

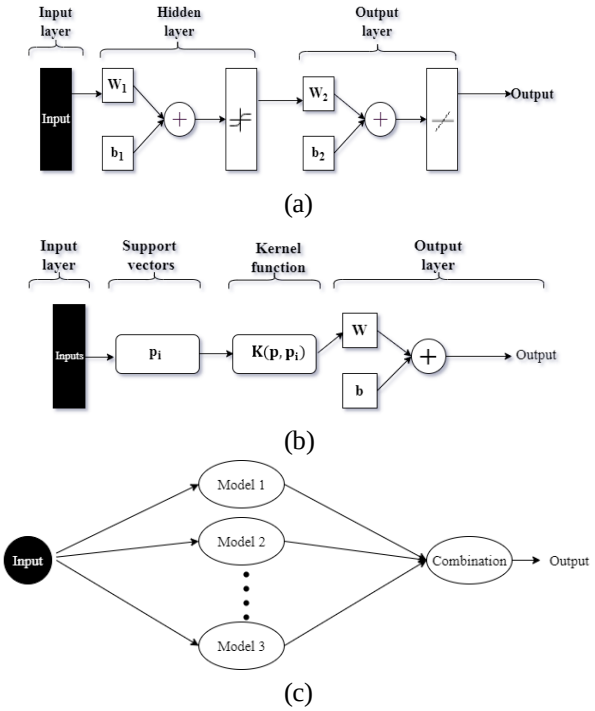

Fig. 2: Structures of the machine learning methods: (a): ANN, (b): SVM, and (c): Ensemble learning

With the help of the defined kernel function for a nonlinear decision boundary, greater flexibility is achieved for the algorithm [34]. This study developed SVM models with linear kernels for the defined regression problem. Fig. 2b shows the structure of the SVM.

Ensemble learning

Ensemble learning is a form of hybrid learning system in which multiple learning models are combined intelligently in order to obtain more accurate and more robust results than a single model. In this study, to perform ensemble learning, a bootstrap aggregating (bagging) method was developed. During this process, random sets of samples were drawn 30 times with replacement, and regression trees were created from these subsets. Replacement is crucial as it ensures that each possible decision tree branching has an equal probability of being represented in the ensemble[32]. This is performed to provide optimal coverage of the domain space. Each newly generated learning set is used as an input to the learning model. Therefore, a series of different hypotheses employed for predicting the value of a dependent variable by combining all generated hypotheses has been obtained. This process was repeated 30 times, after which the models from the samples were combined by averaging the output for regression. Bagging excels when unstable-based algorithms with high variances, such as regression trees, are used. Bagging is robust since increasing the number of generated hypotheses does not lead to overfitting the overall algorithm. The minimum leaf size and the number of learning cycles were set at 8 and 30, respectively. The method of bagging was Bootstrap aggregating. Fig. 2 c demonstrates the architecture of the ensemble learning method.

RESULTS AND DISCUSSION

In order to predict CH_4 conversion, CO_2 removal, and H_2 purity of a SECLR unit, three different machine learning methods were utilized, namely Artificial Neural Network (ANN), ensemble learning, and SVM.

Fig. 3a depicts the comparison between ANN predicted and experimental CH_4 conversion. Also, Fig. 3b shows the ensemble learning prediction *vs.* experimental CH_4 conversion. In addition, Fig. 3c indicates the analogy between the prediction of SVM for CH_4 conversion and the experimental values.

As observed, ANN provides a better convergence between predicted and experimental CH_4 conversion. Fig. 3d shows the distribution of error of ANN prediction for CH_4 conversion. The interval of error for ANN falls between [-0.1363, 0.0947] and [-0.1319, 0.0872] for the train set and test set, respectively. Fig. 3e depicts the ensemble learning error distribution for the prediction of CH_4 conversion. As seen, the error interval for ensemble learning falls between [-0.1608, 0.0778], and [-0.1529, 0.0796] for train set and test set, respectively. Fig. 3f depicts the attributed error distribution to SVM for the prediction of CH_4 conversion. As can be seen, the interval of error for SVM falls between [-0.1967, 0.0972], and [-0.1931, 0.0967] for the train set and test set, respectively. By comparing the intervals of the machine learning methods, it can be found that ANN has the narrowest error distribution due to the high accuracy of ANN in predicting the CH4 conversion. Moreover, according to table 3 for CH4 conversion prediction, ANN provided the least MSE, RMSE, and highest R2 compared to ensemble learning and SVM.

Fig. 4a shows the comparison between ANN predicted and experimental CO_2 removal. Also, fig. 4b indicates the ensemble learning prediction vs. experimental CO_2 removal. Moreover, fig. 4c depicts the analogy between the prediction of SVM for CO_2 removal and the experimental values. As it can be seen, ANN provides a better convergence between predicted and experimental

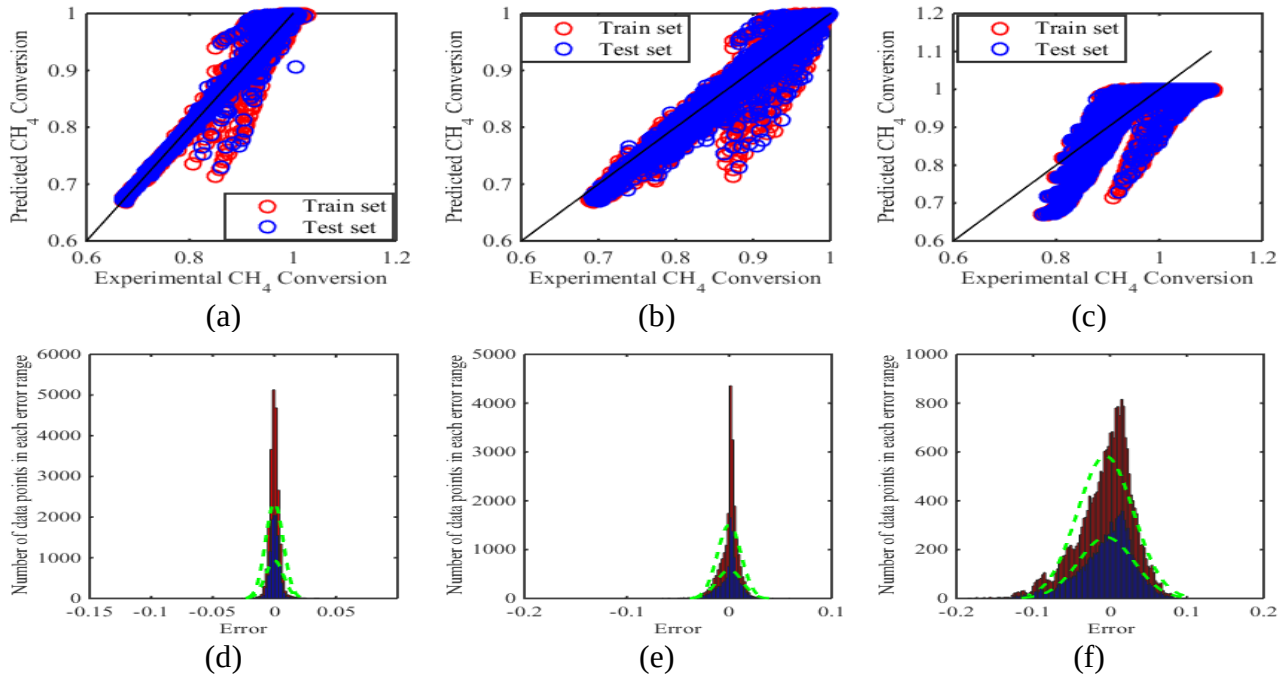

Fig. 3: The machine learning resulted obtained for predicting CH4 conversion: (a) comparison between experimental and ANN predicted values, (b) comparison between experimental and ensemble predicted values, (c) comparison between experimental and SVM predicted values, (d) error distribution of ANN predicted values, (e) error distribution of ensemble predicted values, and (f) error distribution of SVM predicted values.

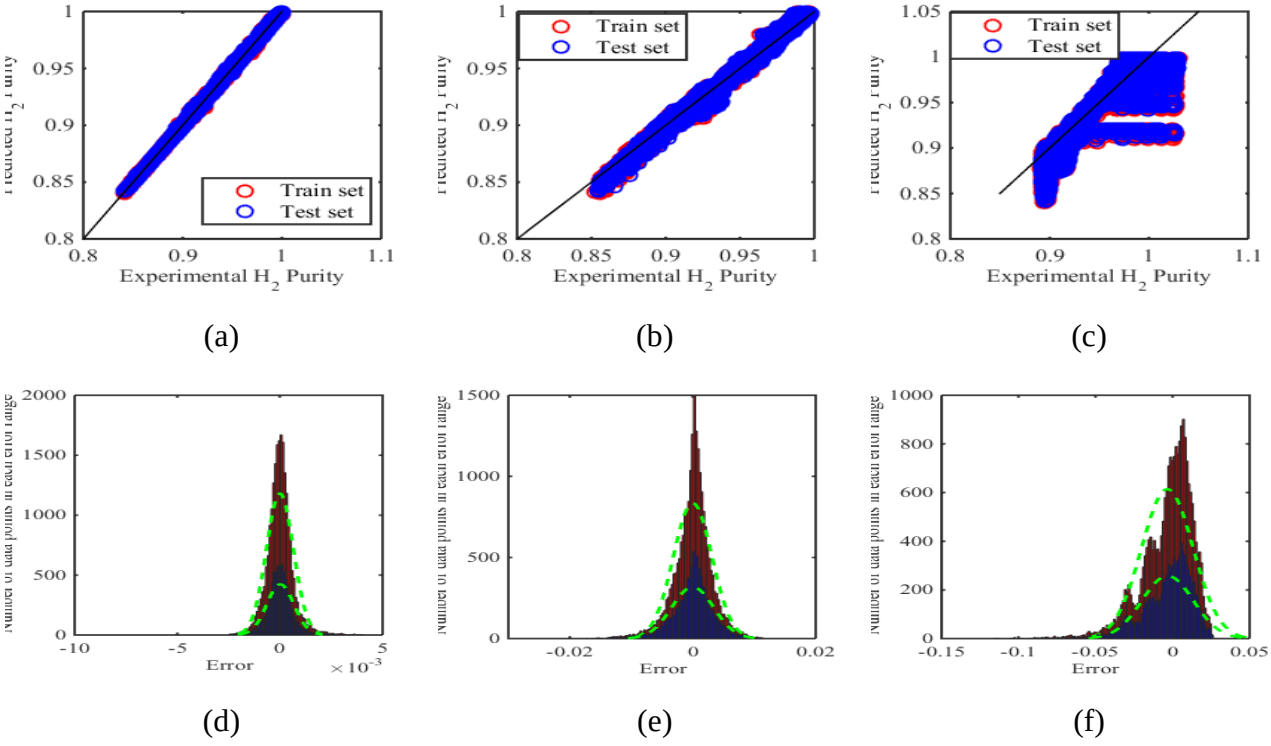

Fig. 4. The machine learning resulted obtained for predicting H2 purity: (a) comparison between experimental and ANN predicted values, (b) comparison between experimental and ensemble predicted values, (c) comparison between experimental and SVM predicted values, (d) error distribution of ANN predicted values, (e) error distribution of ensemble predicted values, and (f) error distribution of SVM predicted values.

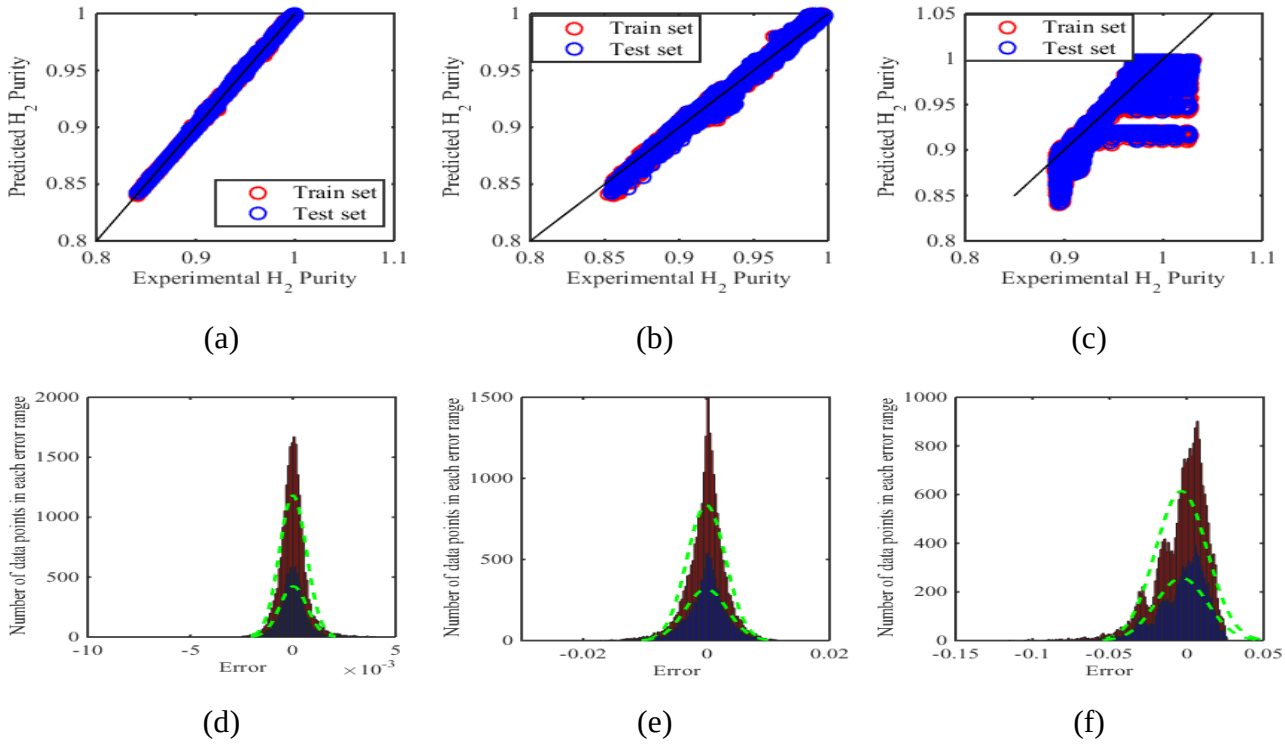

Fig. 5. The machine learning resulted obtained for predicting H2 purity: (a) comparison between experimental and ANN predicted values, (b) comparison between experimental and ensemble predicted values, (c) comparison between experimental and SVM predicted values, (d) error distribution of ANN predicted values, (e) error distribution of ensemble predicted values, and (f) error distribution of SVM predicted values.

CO_2 removal. Fig. 4d exhibits the distribution of error of ANN prediction for CO_2 removal. The interval of error for ANN falls between [-0.0120, 0.0121], and [-0.0087, 0.0119] for the train set and test set, respectively. Fig. 4e displays the ensemble learning error distribution for the prediction of CO_2 removal. As observed, the error interval for ensemble learning falls between [-0.0471, 0.0254] and [-0.0489, 0.0249] for the train set and test set, respectively. Fig. 4f shows the related error distribution to SVM for the prediction of CO_2 removal. As seen, the error interval for SVM falls between [-0.1595, -0.0487], and [-0.1567, 0.0473] for the train set and test set, respectively. Comparing the intervals of the machine learning methods shows that ANN has the narrowest error distribution due to its high accuracy in predicting CO_2 removal. Furthermore, according to table 3 for CO_2 removal prediction, ANN provided the least MSE, RMSE, and highest R^2. In comparison with ensemble learning and SVM.

Fig. 5a depicts the comparison between ANN predicted and experimental H_2 purity. Also, Fig. 5b shows the ensemble learning prediction vs. experimental H_2 purity. Furthermore, Fig. 5c depicts the analogy between the prediction of SVM for H_2 purity and the experimental values. As it can be seen, ANN provides a better convergence between predicted and experimental H_2 purity. Fig. 5d displays the distribution of error of ANN prediction for H_2 purity. The interval of error for ANN falls between [-0.006, 0.0046], and [-0.0045, 0.0044] for the train set and test set, respectively. Fig. 5e displays the ensemble learning error distribution for the prediction of H_2 purity. As observed, the error interval for ensemble learning falls between [-0.0197, 0.0163] and [-0.0203, 0.0145] for the train set and test set, respectively. Fig. 5f shows the related error distribution to SVM for the prediction of CO_2 removal. As can be seen, the interval of error for SVM falls between [-0.1149, -0.0267] and [-0.1121, 0.0259] for the train set and test set, respectively. Comparing the intervals of the machine learning methods shows that ANN has the narrowest error distribution due to the high accuracy of ANN in predicting the H_2 purity. Furthermore, according to table 4 for H_2 purity prediction, ANN provided the least MSE, RMSE, and highest R2 compared to ensemble learning and SVM.

Table 4: Statistical analysis on the performance of developed models

Output	Model	MSE		RMSE		R^2	
		Train	Test	Train	Test	Train	Test
CH_4 conversion (%)	ANN	5.16e-5	5.4e-5	0.0072	0.0073	0.9896	0.9889
	Ensemble	1.33e-4	1.5e-4	0.0115	0.0123	0.9775	0.9734
	SVM	0.0014	0.0013	0.0317	0.0364	0.7312	0.7342
CO_2 removal (%)	ANN	2.32e-6	2.41e-6	0.0015	0.0016	0.9989	0.9989
	Ensemble	5.024e-5	6.04e-5	0.0071	0.0081	0.9852	0.9821
	SVM	6.55e-4	6.87e-4	0.0256	0.0262	0.7206	0.7240
H_2 Purity (%)	ANN	4.32e-7	4.36e-7	6.57e-4	6.61e-4	0.9996	0.9996
	Ensemble	9.82e-6	1.63e-5	0.0031	0.0034	0.9941	0.9928
	SVM	2.91e-4	2.82e-4	0.0171	0.0170	0.7735	0.7742

CONCLUSIONS

In this paper, an AI-based modeling of a SECLR unit was accomplished. To this end, first a SECLR unit was simulated via ASPEN Plus and then validated by experimental data. Afterward, ASPEN validated simulation was conducted under 31000 different scenarios in terms of different operational conditions. The data obtained from ASPEN plus was used to develop prediction models with machine learning methods. Artificial neural network, ensemble learning, and SVM methods were developed to predict the CH4 conversion, CO_2 removal, and H_2 Purity of a SECLR unit. The performance and accuracy of machine learning developed R2, MSE, and RMSE measured models. ANN presented the best performance to predict CH_4 conversion, CO_2 removal, and H_2 Purity among all three machine learning methods. For CH_4 conversion, the R2 of ANN is 0.9896 and 0.9889 for the train set and test set, respectively. Also, in the prediction of CH_4 conversion, ANN provides MSE of 5.16e-5 and 5.4e-5 for the train set and test set, respectively. Moreover, the estimation of CH_4 conversion via ANN led to an RMSE of 0.0072 and 0.0073 for the train set and test set, respectively. For CO_2 removal, the R2 of ANN is 0.9852 and 0.9821 for the train set and test set, respectively. Also, in the prediction of CO_2 removal, ANN provides MSE of 5.024e-5 and 6.04e-5 for the train set and test set, respectively. Moreover, the estimation of CO_2 removal via ANN led to an RMSE of 0.0071 and 0.0081 for the train and test sets, respectively. For H_2 Purity, R2 of ANN is 0.9996 and 0.9998 for the train set and test set, respectively. Also, in the prediction of H_2 Purity, ANN provides MSE of 4.32e-7 and 4.36e-7 for the train set and test set, respectively. Moreover, the estimation of H_2 Purity via ANN led to RMSE of 0.0031 and 0.0034 for the train and test sets, respectively. Finally, in the AI-based modeling of this paper time is not considered. A suggestion to extend this work is to investigate the time-series prediction of the SECLR unit using recurrent neural networks.

Received : Aug. 09, 2022 ; Accepted : Nov. 23 , 2022

REFERENCES

[1] Cerqueira P., Soria M., Madeira L.M., Hydrogen Production through Chemical Looping and Sorption-Enhanced Reforming of Olive Mill Wastewater, *Thermodynamic and Energy Efficiency Analysis. Energy Conversion and Management*, **238**: 114146. (2021).

[2] Mutlu A.Y., Yucel O., An Artificial Intelligence Based Approach to Predicting Syngas Composition for Downdraft Biomass Gasification, *Energy*,. **165**: 895-901 (2018).

[3] Kalamaras C.M., Efstathiou A.M., "Hydrogen Production Technologies: Current State and Future Developments", In *Conference Papers In Science*., Hindawi (2013).

[4] Powell J., et al., Optimisation of a Sorption-Enhanced Chemical Looping Steam Methane Reforming Process, *Chemical Engineering Research and Design*,. **173**:183-192 (2021).

[5] Norouzi N., Kalantari G., Talebi S., Combination of Renewable Energy in the Refinery, with Carbon Emissions Approach, *Biointerface Res. Appl. Chem.*, **10(4)**: 5780-5786 (2020).

[6] Norouzi N., et al., Heavy Oil Thermal Conversion and Refinement to the Green Petroleum: a Petrochemical refinement plant using the Sustainable Formic Acid for the Process, *Biointerface Res. Appl. Chem.*, **10(5)**: 6088-6100 (2020).

[7] Kartal F., Özveren U., A Deep Learning Approach for Prediction of Syngas Lower Heating Value from CFB Gasifier in Aspen Plus, *Energy*., **209**: 118457 (2020).

[8] Zhao Y., et al., Thermodynamic Analysis of a New Chemical Looping Process for Syngas Production with Simultaneous CO_2 Capture and Utilization, *Energy Conversion and Management*, **171**: 1685-1696 (2018).

[9] Saithong N., et al., Thermodynamic Analysis of the Novel Chemical Looping Process for Two-Grade Hydrogen Production with CO_2 Capture**,** *Energy Conversion and Management*, **180**: 325-337 (2019).

[10] Mattisson T., Lyngfelt A., Applications of Chemical-Looping Combustion with Capture of CO_2**,** Second Nordic Minisymposium on CO_2 Capture and Storage, Göteborg, Sweden, (2001).

[11] Di Z., et al., Thermodynamic Analysis on the Parametric Optimization of a Novel Chemical Looping Methane Reforming in the Separated Productions of H_2 and CO**,** *Energy Conversion and Management*, **192**: 171-179 (2019).

[12] Zhang Q., et al., Multifunctional Ni-Based Oxygen Carrier for H_2 Production by Sorption Enhanced Chemical Looping Reforming of Ethanol**,** *Fuel Processing Technology*, **221**: 106953 (2021).

[13] Li F., et al., Modelling of a Post-Combustion CO_2 Capture Process Using Neural Networks, *Fuel*, **151**: 156-163 (2015).

[14] Khajehpour H., Norouzi N., Fani M., An Exergetic Model for the Ambient Air Temperature Impacts on the Combined Power Plants and its Management Using the Genetic Algorithm, *International Journal of Air-Conditioning and Refrigeration*, **29**: (2021).

[15] Norouzi N., et al., A 4E Analysis of Renewable formic Acid Synthesis from the Electrochemical Reduction of Carbon Dioxide and Water: Studying Impacts of the Anolyte Material on the Performance of the Process, *Journal of Cleaner Production*, **293**: 126149 (2021).

[16] Norouzi N., et al., Energy, Exergy, and Exergoeconomic (3E) Analysis of Gas Liquefaction and Gas Associated Liquids Recovery Co-Process Based on the Mixed Fluid Cascade Refrigeration Systems, *Iran. J. Chem. Chem. Eng. (IJCCE)*, **41(4):** 1391-1410 (2022).

[17] Norouzi N., Talebi S., Exergy, Economical and Environmental Analysis of a Natural Gas Direct Chemical Looping Carbon Capture and Formic Acid-Based Hydrogen Storage System, *Iranian Journal of Chemistry and Chemical Engineering (IJCCE)*, **41(4):** 1436-1457 (2022).

[18] Norouzi N., Hydrogen Production in the Light of Sustainability: A Comparative Study on the Hydrogen Production Technologies Using the Sustainability Index Assessment Method, *Nuclear Engineering and Technology*, **54(4)**: 1288-1294 (2022).

[19] Norouzi N., *The Pahlev Reliability Index:* A Measurement for the Resilience of Power Generation Technologies Versus Climate Change, *Nuclear Engineering and Technology*, **53(5)**: 1658-1663 (2021).

[20] Norouzi N., Fani M., Talebi S., Exergetic Design and Analysis of a Nuclear SMR Reactor Tetrageneration (Combined Water, Heat, Power, and Chemicals) with Designed PCM Energy Storage and a CO_2 Gas Turbine Inner Cycle, *Nuclear Engineering and Technology*, **53(2)**: 677-687 (2021).

[21] Khajehpour H., et al., Exergy Analysis and Optimization of Natural Gas Liquids Recovery Unit, I*nternational Journal of Air-Conditioning and Refrigeration*, **29(01)**: 2150005 (2021).

[22] Norouzi N., Shiva N., Khajehpour H., Optimization of Energy Consumption in the Process of Dehumidification of Natural Gas, B*iointerface Research in Applied Chemistry*, **11**: 14634-14639 (2021).

[23] Norouzi N., et al., Exergy and Exergoeconomic Analysis of Hydrogen and Power Cogeneration Using an HTR Plant, *Nuclear Engineering and Technology*, **53(8)**: 2753-2760 (2021).

[24] Norouzi N., H Khajehpour, Simulation of Methane Gas Production Process from Animal Waste in a Discontinuous Bioreactor, *Biointerface Research in Applied Chemistry*, **11**:13850-13859 (2021).

[25] Norouzi N., Talebi S., Najafi P., Thermal-Hydraulic Efficiency of a Modular Reactor Power Plant by Using the Second Law of Thermodynamic, *Annals of Nuclear Energy*, **151**:107936 (2021).

[26] Khajehpour H., Norouzi N., Fani M., An Exergetic Model for the Ambient Air Temperature Impacts on the Combined Power Plants and its Management Using the Genetic Algorithm**,** I*nternational Journal of Air-Conditioning and Refrigeration*, **29(01)**: 2150008 (2021).

[27] Norouzi N., 4E Analysis and Design of a Combined Cycle with a Geothermal Condensing System in Iranian Moghan Diesel Power Plant, *International Journal of Air-Conditioning and Refrigeration*, **28(03)**: 2050022 (2020).

[28] Shalaby A., et al., A Machine Learning Approach for Modeling and Optimization of a CO Post-Combustion Capture Unit, *Energy*, **215**: 119113 (2021).

[29] Bai Z., et al., Modelling of a Post-Combustion CO_2 Capture Process Using Bootstrap Aggregated Extreme Learning Machines**,** in "Computer Aided Chemical Engineering", Elsevier. 2007-2012 (2016).

[30] Valera V.Y., Codolo M.C., Martins T.D., Artificial Neural Network for Prediction of SO_2 Removal and Volumetric Mass Transfer Coefficient in Spray Tower**,** *Chemical Engineering Research and Design*, **170**:1-12 (2021).

[31] Rydén M., Ramos P., H_2 Production with CO_2 Capture by Sorption Enhanced Chemical-Looping Reforming Using NiO as Oxygen Carrier and CaO as CO_2 Sorbent**,** *Fuel Processing Technology*,. **96**: 27-36 (2012).

[32] Elmaz F., Yücel Ö., Mutlu A.Y., Predictive Modeling of Biomass Gasification with Machine Learning-Based Regression Methods, *Energy*, **191**: 116541 (2020).

[33] Ahmad, I., et al., Machine Learning Applications in Biofuels' Life Cycle: Soil, Feedstock, Production, Consumption, and Emissions**,** *Energies*, **14(16)**: 5072 (2021).

[34] Nkulikiyinka P., et al., Prediction of Sorption Enhanced Steam Methane Reforming Products from Machine Learning Based Soft-Sensor Models, *Energy and AI*, **2**:100037 (2020).